A Thermodynamic Equation of State for Pentafluoroethane (R-125)

H. Sunaga[2], R. Tillner-Roth[3], H. Sato[2,4], and K. Watanabe[2]

---

[1] Paper presented at the Thirteenth Symposium on Thermophysical Properties, June 22-27, 1997, Boulder, Colorado, USA.

[2] Department of System Design Engineering, Faculty of Science and Technology, Keio University, 3-14-1 Hiyoshi, Kohoku-ku, Yokohama 223, Japan.

[3] Institute of Thermodynamics, University of Hannover, Callinstrasse 36, 30167, Hannover, Germany.

[4] Author to whom correspondence should be addressed.

ABSTRACT

Pentafluoroethane (R-125, CHF_2CF_3), one of hydrofluorocarbons, is an environmentally acceptable refrigerant and expected to be a promising component of binary and ternary mixture refrigerants to replace R-22 due to its zero ODP (ozone depletion potential) and its non-flammability. The accurate knowledge of its thermodynamic properties is essential to develop equations of state for the mixtures. We developed an equation of state for R-125 which is a fundamental equation of state represented as a non-dimensional Helmholtz free energy. The equation has been established on the basis of the selected measurements on the pressure-density-temperature (P, ρ, T), speed of sound, heat capacities, and the saturation properties. Linear and non-linear regression procedures were used to determine the functional form and the numerical parameters of the fundamental equation of state. The equation represents all the thermodynamic properties of R-125 in the liquid and the gaseous phases for temperatures between the triple-point and 470 K, and pressures up to 35 MPa.

KEY WORDS: equation of state; HFCs ; pentafluoroethane ; R-125; refrigerant; thermodynamic properties

1. INTRODUCTION

Hydrofluorocarbons (HFCs) are the most promising environmentally-safe refrigerants for replacing ozone depleting refrigerants which include chlorine atom such as chlorodifluoromethane (R-22) for the refrigerant in most of air-conditioning systems or azeotrope mixture refrigerants (R-502) of 48.8 mass% R-22 and 51.2 mass% chloropentafluoroethane (R-115) for the refrigerant in large-scale commercial refrigeration units. The HFCs include pure and mixture refrigerants of trifluoromethane (R-23), difluoromethane (R-32), pentafluoroethane (R-125), 1,1,1,2-tetrafluoroethane (R-134a), 1,1,1-trifluoroethane (R-143a), and 1,1-difluoroethane (R-152a). Among these HFCs, the binary and ternary mixture refrigerants of R-32, R-125, R-134a, and R-143a are becoming the realistic alternative refrigerants to R-22 and R-502 at present.

The thermodynamic equations of state(EOS) for the pure and mixture HFCs are necessary to be developed for providing the fundamental information to air-conditioning and refrigeration industries. The EOS for pure R-134a and R-32 have already been developed by Tillner-Roth, one of the present authors, and Baehr[1] and by Tillner-Roth and Yokozeki[2]. Both of them are accepted as the international EOS by the IEA(International Energy Agency)-Annex XVIII. We have already developed the EOS for not only pure R-125 and R-143a but also the binary and ternary mixtures of these HFCs. The paper on the EOS of R-143a is also prepared by Li et al.[3] in our group and the preparation of the papers for the EOS for mixture refrigerants is in progress.

This paper reports the EOS for R-125 which is based on the selected accurate experimental data and the thermodynamic properties including the specific heats and speeds of sound are reasonably represented even in the region where no reliable experimental data exist at temperatures between 172.52 K (triple point) and 470 K, and pressures up to 35 MPa by the present EOS.

The detailed method of regression analysis is not possible to be described in this paper due to a page limitation. The method used in the present study was the same one

used by Tillner-Roth and Baehr[1] in the process of the development of the EOS of R-134a. The experimental data on the thermodynamic properties of R-125, the functional form and the numerical parameters of the present equation, the comparison of the EOS with the selected experimental data, and the behavior of constant-pressure lines of the specific heats and the speed of sound are presented in this paper.

2. AVAILABLE EXPERIMENTAL DATA

The selected data mainly used for establishing the EOS of R-125 are listed in Table I and the data-point distribution is shown in a *PT*-diagram(Fig. 1) and a $T\rho$-diagram(Fig. 2). Although more than 4,500 experimental data have been measured for R-125, we did not use all of them but carefully evaluated and selected the data. A part of 4,500 experimental data have been reported in the academic papers, but the remainder of them have not been published yet. Members of IEA-Annex XVIII who are developing the EOS are exchanging each other via internet regarding the information on the experimental data compiled on a common data-file in a computer at the University of Stuttgart.

Accurate density data were reported for temperatures between 180 K and 413 K and pressures up to 70 MPa covering the liquid and the vapor phases, densities up to 1700 kg·m^{-3}. Accurate vapor pressure measurements cover the wide temperature range up to the critical temperature and accurate heat-capacity and speed-of-sound measurements are also available as shown in Table I. The quality and quantity of the experimental data are sufficient for developing a reliable EOS for R-125.

3. THERMODYNAMIC EQUATION OF STATE

The thermodynamic equation of state for R-125 is a non-dimensional Helmholtz free energy with two independent variables, reduced density δ and reduced inverse temperature τ.

$$\Phi(\tau,\delta) = \frac{A_m}{R_m T} = \frac{A}{RT} = \Phi^0(\tau,\delta) + \Phi^r(\tau,\delta) \qquad (1)$$

where R_m = 8.314471 J·mol^{-1}·K^{-1} is the universal gas constant reported by Moldover et

al.[4]; A_m is the molar Helmholtz free energy; A is the specific free energy; $R = R_m / M$ is the individual gas constant where the molar mass is M = 120.022 g·mol^{-1}. Independent variables τ and δ are

$$\tau = T_c / T \qquad \text{and} \qquad \delta = \rho / \rho_c \tag{2}$$

where T_c = 339.165 K and ρ_c = 568 kg·m^{-3} are critical parameters determined by Kuwabara et al.[5] and recommended by Higashi[6]. The non-dimensional Helmholtz free energy Φ consists of an ideal-gas part Φ^0 and a residual part Φ^r. The ideal-gas part Φ^0 was initially determined on the basis of the values theoretically determined by Yokozeki et al.[7,8]. The numerical parameters of Φ^0 were readjusted in the procedure for determining those of the residual part Φ^r by fitting it to all the thermodynamic property data not only in the single phase but those at the vapor-liquid equilibrium states. The equation of the ideal-gas part Φ^0 is finally determined as,

$$\Phi^0(\tau,\delta) = a_1^0 + a_2^0\tau + a_3^0 \ln\tau + \sum_{i=1}^{3} m_i^0 \ln\left[1 - \exp\left(-\theta_i^0 \tau\right)\right] + \ln\delta \tag{3}$$

where the coefficients are

$$a_1^0 = -12.9469, \quad a_2^0 = 8.512891, \quad a_3^0 = 4.911212,$$

$$m_1^0 = 6.856764, \quad m_2^0 = 4.885985, \quad m_3^0 = 3.292859,$$

$$\theta_1^0 = 1.9757425, \quad \theta_2^0 = 4.7965398, \quad \theta_3^0 = 5.4932421 \ .$$

The coefficients of a_1^0 and a_2^0 were determined by assigning the enthalpy and the entropy values for the saturated liquid at 273.15 K being h = 200 kJ·kg^{-1} and s = 1 kJ·kg^{-1}·K^{-1}, respectively.

Two optimization strategies, linear and non-linear optimization procedures, were applied to determine the functional form and the numerical parameters by mainly fitting the selected experimental data listed in Table I. Further information on the optimization process is given by Tillner-Roth and Baehr[1,9]. The functional form of the residual part Φ^r is determined as,

$$\Phi^{\mathrm{r}}(\tau,\delta)=\sum_{\mathrm{i}=1}^{5}a_{\mathrm{i}}\tau^{t_{\mathrm{i}}}\delta^{d_{\mathrm{i}}}+\exp(-\delta)\sum_{\mathrm{i}=6}^{12}a_{\mathrm{i}}\tau^{t_{\mathrm{i}}}\delta^{d_{\mathrm{i}}}$$
$$+\exp\left(-\delta^{2}\right)\sum_{\mathrm{i}=13}^{16}a_{\mathrm{i}}\tau^{t_{\mathrm{i}}}\delta^{d_{\mathrm{i}}}+\exp\left(-\delta^{3}\right)\sum_{\mathrm{i}=17}^{18}a_{\mathrm{i}}\tau^{t_{\mathrm{i}}}\delta^{d_{\mathrm{i}}} \quad (4)$$

The coefficients a_{i} and exponents t_{i} and d_{i} are listed in Table II.

4. COMPARISON WITH AVAILABLE EXPERIMENTAL DATA

Table III shows the experimental data in the publications. Unpublished data are not listed in Table III. The species of the properties, the number of data points, the mean deviation (bias), and the standard deviation are listed in Table III. The measured ranges and the experimental uncertainties of the selected experimental data used for developing the EOS for R-125 are summarized in Table I.

Figure 3 shows the comparison of ideal-gas heat-capacity values with theoretical values determined by Yokozeki et al.[7] and the values determined on the basis of the speed-of-sound measurements by Gillis[18]. Those values agree with each other within ±0.2 %. The present ideal-gas part equation can represent most of the values derived by Yokozeki et al.[7] within ±0.1 %.

Regarding the saturation properties, the vapor pressure values agree with the measurements of de Vries[10] in the temperature range from 220 K to the temperature near the critical temperature within ±0.2 kPa as shown in Fig. 4, whereas the saturated-liquid-density values agree with the measurements of Magee[11], Defibaugh[15], and Widiatmo[19] at temperatures from 170 K to 330 K within ±0.2 % as shown in Fig. 5.

Regarding the density values in the gaseous phase, the EOS represents the selected data (expect 13 data very near the saturation state or the critical point) within ±0.1 % at the density range from 0 to 600 kg·m^{-3}and the EOS represents most of the density data in the liquid phase within ±0.1 %.

Speed of sound measurements by Gillis[18] in the gaseous phase are well reproduced within ±0.025 %, while those of Grebenkov et al.[17] in the liquid phase are reproduced within ±0.5 %. Specific heat capacities at constant volume measured by

Lueddecke and Magee[16] are reproduced within ±1 % at temperatures between 200 K and 340 K by the present EOS.

5. HEAT CAPACITIES AND SPEED OF SOUND

A severe test for checking the reliability of the EOS is the calculation of the heat capacities and the speed of sound thermodynamic surfaces from the EOS. Figures 6 and 7 show the behavior of the constant pressure lines between 50 kPa and 100 MPa for the specific heat capacity at constant pressure and the speed of sound derived from the present EOS, respectively. At temperatures between 170 K and 570 K, the thermodynamic surfaces for these properties are confirmed as being physically correct. Although the effective range of the present EOS is for temperatures up to 470 K and pressures up to 35 MPa, the present EOS is possible to be used for the prediction of the thermodynamic properties beyond the effective range up to 570 K and 100 MPa.

6. CONCLUSION

The present equation of state for R-125 is valid for temperatures from 172.52 K(the triple point temperature) to 470 K, pressures up to 35 MPa, and densities up to 1700 $kg \cdot m^{-3}$. The reliability of the present EOS can be estimated better than ±0.1% for density values in the entire effective range and the thermodynamic properties calculated from the present EOS are satisfactorily represented for the prediction in the extensive range up to 570 K in temperature and up to 100 MPa in pressure from physical viewpoint.

ACKNOWLEDGMENTS

The authors thank Prof. Yokozeki and Mr. Li for their valuable comments and discussions on the ideal-gas heat-capacity values and general problems for developing the present EOS. The authors are grateful to the New Energy and Industrial Technology Development Organization (NEDO), Tokyo, for the financial support to the present study.

REFERENCES

1. R. Tillner-Roth and H. D. Baehr, *J. Phys. Chem. Ref. Data.* **23**: 657 (1994).
2. R. Tillner-Roth and A. Yokozeki, to be submitted for *J. Phys. Chem. Ref. Data*: (1997).
3. J. Li, R. Tillner-Roth, H. Sato and K. Watanabe, to be submitted for *Int. J. Thermophys*. (1997).
4. M. R. Moldover, J. P. M. Trusler, T. J. Edwards, J. B. Mehl and R. S. Davis, *J. Res. Natl. Bur. Stand.* **93**: 85 (1988).
5. S. Kuwabara, H. Aoyama, H. Sato and K. Watanabe, *J. Chem. Eng. Data.* **40**: 112 (1995).
6. Y. Higashi, *Proc. of 1996 JAR Annual Conf. Nov. 13-15, Fukuoka*: 97 (1996).
7. A. Yokozeki, H. Sato and K. Watanabe, to be submitted for *Int. J. Thermophys*.
8. A. Yokozeki, H. Sato and K. Watanabe, paper to be presented at the *Symp. on Thermophys. Props., Boulder, Colorado, June 22-27*, (1997).
9. R. Tillner-Roth, Forsch. Ber. DKV Nr. 41, DKV, Stuttgart (1993).
10. B. deVries, *Dissertation, Universiaet Hannover*, Germany, (1996).
11. J. V. Magee, *Int. J. Thermophysics*, **17**: 803 (1994).
12. H. -L. Zhang, H. Sato and K. Watanabe, *Proc. of 19th Int. Cong. Refrig.* , **IVa**: 622 (1995); Numerical data provided as private communication.
13. S. J. Boyes and L. A. Weber, *J. Chem. Thermodyn.* **27**: 163 (1995).
14. H. A. Duarte-Garza, C. -A. Hwang, B. E. Gammon, K. N. Marsh, K. R. Hall, and J. C. Holste, *ASHRAE Trans.* , **99, Part 2**: 649 (1993).
15. D. R. Defibaugh and G. Morrison, *Fluid Phase Equilibria* **80**: 157 (1992).
16. T. O. Lueddecke and J. V. Magee, *Int. J. Thermophysics.* **17**: 823 (1994) .
17. A. J. Grevenkov, O. V. Beljiava,T. A. Zajatz, and B. D. Timofeev, *Proc. of 4th Asian Thermophys. Prop. Conf.* , **2**: 311 (1995).
18. K. A. Gillis, to be submitted for *Int. J. Thermophys*. (1996).
19. J. V. Widiatmo, H. Sato and K. Watanabe, *J. Chem. Eng. Data.* **39**: 304 (1994).
20. L. A. Weber and A. M. Silva, *J. Chem. Eng. Data.* **39**: 808 (1994).

Table I. Selected Experimental Data for R-125

First author	Year	Property	P Range/MPa	δP / kPa	ρ / kg m^{-3} Range	$\delta\rho$	T / K Range	δT	Data points	Ref.
deVries	1996	*PVT*	0.03 - 19	0.02%	3.8 - 1189	0.4	263 - 393	0.01	367	[10]
deVries	1996	*PVT*	1 - 18	0.01%	151 - 1509	0.03%	243 - 413	0.01	595	[10]
Magee	1996	*PVT*	3.5 - 35	0.05%	1114 - 1683	0.05%	178 - 398	0.03	97	[11]
Zhang	1995	*PVT*	0.1 - 3.6	0.8	4.9 - 229	0.12%	290 - 390	0.01	93	[12]
Boyes	1994	*PVT*	0.3 - 5	0.17	0.3 - 4.6	0.36	260 - 350	0.001	80	[13]
Duarte-Garza	1994	*PVT*	1.2 - 68	10	855 - 1694	0.10%	180 - 350	0.01	151	[14]
Defibaugh	1992	*PVT*	1.6 - 6.3	0.5	258 - 1348	0.05%	275 - 369	0.01	162	[15]
Lueddecke	1996	c_v	3.8 - 33	n.a.	1264 - 1624	n.a.	200 - 341	n.a.	97	[16]
Grebenkov	1995	*W*	1.6 - 16	0.10%	------	------	287 - 332	0.02	30	[17]
Gillis	1994	*W*	0.04 - 1	1	------	------	240 - 400	n.a.	149	[18]
Magee	1996	ρ'	------	------	1124 - 1688	0.10%	173 - 308	0.01	7	[11]
Widiatmo	1994	ρ'	------	------	1286 - 1530	0.2%	220 - 280	0.02	25	[19]
Defibaugh	1992	ρ'	------	------	771 - 1309	0.05	276 - 338	0.01	9	[15]
deVries	1996	P_s	0.09 - 3.6	0.01%	------	------	224 - 339	0.01	100	[10]
Boyes	1995	P_s	0.67 - 3.3	0.15	------	------	273 - 335	0.01	29	[13]
Weber	1994	P_s	0.07 - 0.95	0.02	------	------	219 - 285	0.01	104	[20]

Table II. Coefficients and Exponents of the Residual Part $\Phi^{r}(\tau,\delta)$ for Eq. (1)

i	a_i		t_i	d_i
1	1.2439220	$\times 10^{-1}$	-0.50	1
2	2.7922179	$\times 10^{-1}$	0.00	2
3	-1.1822597	$\times 10^{0}$	1.50	2
4	2.3616512	$\times 10^{-1}$	1.50	3
5	-1.1571810	$\times 10^{-2}$	3.00	2
6	1.225177	$\times 10^{0}$	0.50	1
7	-2.147964	$\times 10^{0}$	1.00	1
8	-2.981380	$\times 10^{-1}$	3.00	1
9	3.391211	$\times 10^{-1}$	2.75	3
10	-6.322995	$\times 10^{-4}$	2.00	8
11	1.271747	$\times 10^{-4}$	-1.00	10
12	5.026962	$\times 10^{-6}$	1.25	12
13	-1.667058	$\times 10^{-1}$	4.00	1
14	-7.332750	$\times 10^{-2}$	4.00	2
15	-6.378780	$\times 10^{-2}$	3.00	4
16	6.833110	$\times 10^{-6}$	0.25	15
17	-1.995426	$\times 10^{-2}$	23.00	3
18	1.260026	$\times 10^{-2}$	14.00	4

Table III. Comparison of the Present EOS with AvailableExperimental Data.

Author	Year	Property	Data points	Mean deviation	Standard deviation	Author	Year	Property	Data points	Mean deviation	Standard deviation
deVries	1996	*PVT*	595	0.05	0.39	deVries	1996	P_s	81	0.01	0.19
deVries	1996	*PVT*	367	0.00	0.17	deVries	1996	P_s	19	0.00	0.03
Magee	1996	*PVT*	97	-0.08	0.05	Lueddecke	1996	P_s	9	-0.04	0.21
Oguchi	1996	*PVT*	167	0.30	1.30	Oguchi	1996	P_s	61	0.05	0.08
Boyes	1995	*PVT*	80	0.05	0.08	Boyes	1995	P_s	29	0.02	0.02
Fukushima	1995	*PVT*	151	-0.56	2.02	Fukushima	1995	P_s	45	-0.02	0.16
Tsvetkov	1995	*PVT*	44	-0.23	0.29	Tsvetkov	1995	P_s	34	0.03	0.05
Zhang	1995	*PVT*	93	0.02	0.10	Duarte-Garza	1994	P_s	15	0.16	0.16
Duarte-Garza	1994	*PVT*	151	-0.12	0.09	Sagawa	1994	P_s	26	0.03	0.03
Monluc	1994	*PVT*	50	-0.66	0.50	Weber	1994	P_s	104	-0.11	0.09
Sagawa	1994	*PVT*	92	0.38	0.29	Widiatmo	1994	P_s	20	-0.27	0.51
Ye	1994	*PVT*	93	0.08	0.12	Ye	1994	P_s	12	0.07	0.04
Baroncini	1993	*PVT*	73	-0.47	0.84	Nagel	1993	P_s	18	0.38	0.23
Defibaugh	1992	*PVT*	162	0.35	2.41	Monluc	1991	P_s	23	-0.05	0.20
Wilson	1990	*PVT*	84	-1.30	3.27	Wilson	1990	P_s	39	0.25	0.54
Magee	1996	ρ'	7	0.02	0.16	Kan	1996	c_P	82	1.90	0.54
Fukushima	1995	ρ'	50	-0.50	1.48	Lueddecke	1996	c_v	97	0.36	0.48
Kuwabara	1995	ρ'	16	0.50	1.01	Lueddecke	1996	$c_v^{(2)}$	97	0.36	0.48
Higashi	1994	ρ'	17	0.12	0.83	Hozumi	1996	W	72	0.03	0.01
Takahashi	1994	ρ'	22	0.09	0.14	Grebenkov	1995	W	30	-0.02	0.21
Widiatmo	1994	ρ'	25	-0.05	0.06	Gillis	1994	W	149	0.00	0.01
Defibaugh	1992	ρ'	9	0.39	1.03	Takagi	1994	W	119	0.84	0.43
						Kraft	1994	W'	13	0.09	0.71
						Kraft	1994	W''	9	-0.23	1.98

[1)] Mean deviation : $\bar{\mathrm{d}} = \frac{1}{N}\sum \mathrm{d}$, $\mathrm{d} = \frac{X_{\mathrm{exp}} - X_{\mathrm{cal}}}{X_{\mathrm{cal}}} \times 100$

[2)] Standard deviation : $\left[\frac{1}{N-1}\sum\left(\mathrm{d}-\bar{\mathrm{d}}\right)^2\right]^{\frac{1}{2}}$

[3)] Deviations for *PVT* properties are given for the density values.

FIGURE CAPTIONS

Fig. 1. Data distribution of the selected experimental data on a pressure-temperature diagram.

◇ Defibaugh and Morrison (1992) + Duarte-Garza et. al. (1994)

△ Boyes and Weber (1995) ○ Zhang et. al. (1995) □ Magee (1996)

× de Vries (1996)

Fig. 2. Data distribution of the selected experimental data on a temperature-density diagram.

◇ Defibaugh and Morrison (1992) + Duarte-Garza et. al. (1994)

△ Boyes and Weber (1995) ○ Zhang et. al. (1995) □ Magee (1996)

× de Vries (1996)

Fig. 3. Comparison of the present EOS regarding the ideal-gas heat-capacities.

□ Gillis (1994) ○ Yokozeki et. al. (1996)

Fig. 4. Comparison of the present EOS regarding the vapor pressure.

○ de Vries (1996)

Fig. 5. Comparison of the present EOS regarding the saturated liquid density.

△ Defibaugh and Morrison (1992) □ Magee (1996)

○ Widiatmo et. al. (1994)

Fig. 6. Constant pressure lines of specific heat capacity at constant pressure derived from the present EOS.

Fig. 7. Constant pressure lines of speed of sound derived from the present EOS.

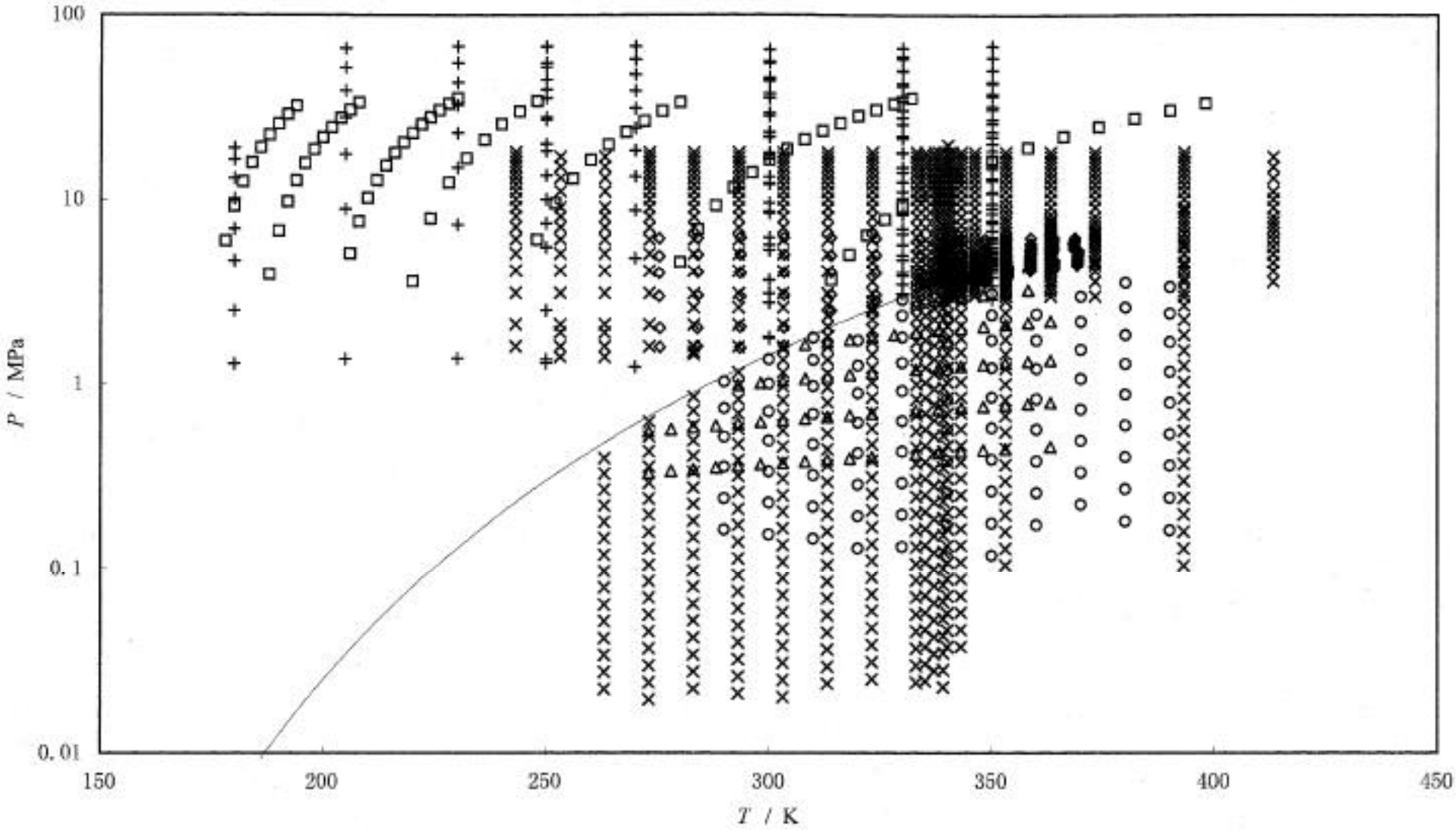

Fig. 1

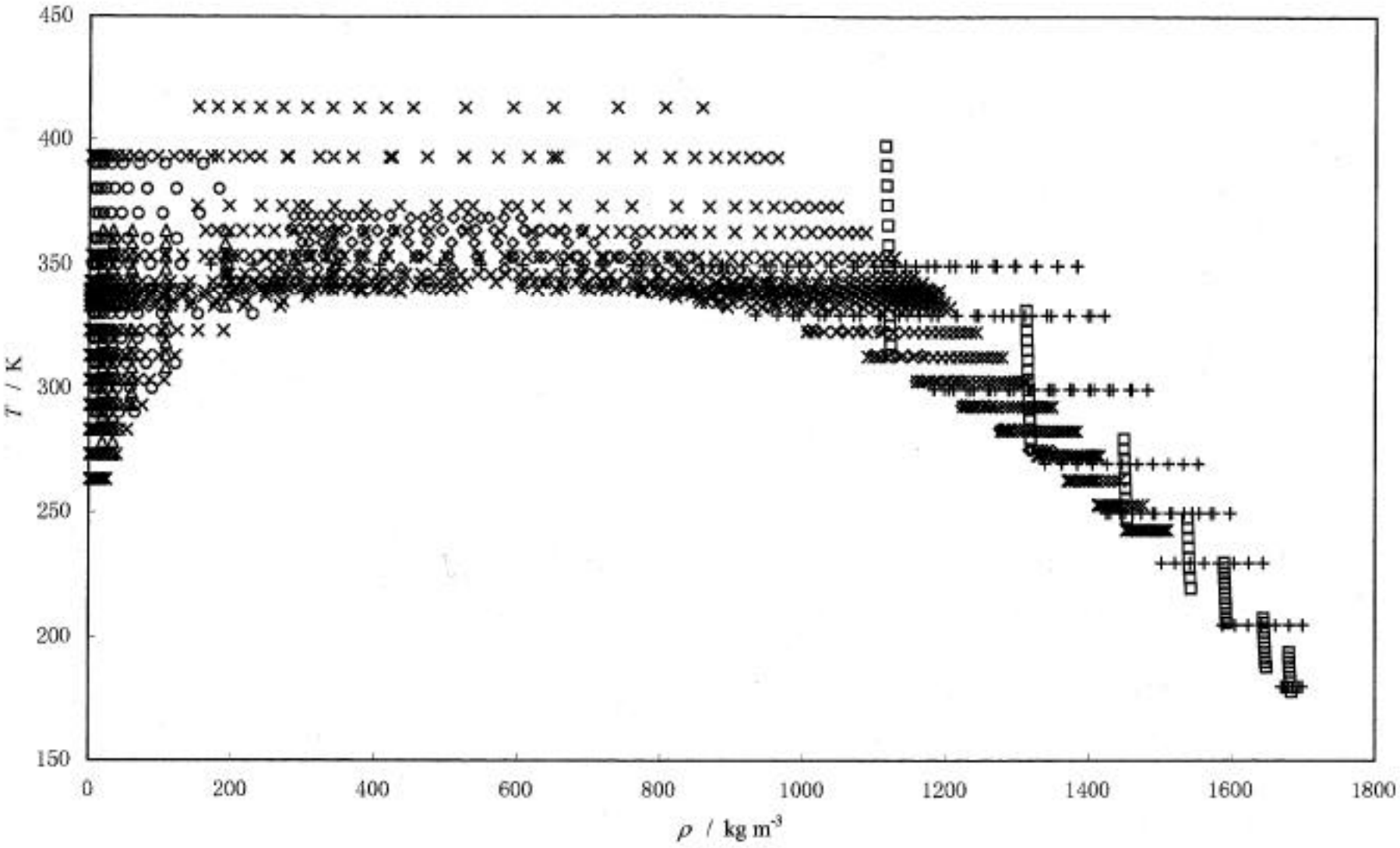
450
400
350
300
250
200
150
T / K
0
200
400
600
800
1000
1200
1400
1600
1800
ρ / kg m-3

Fig. 2

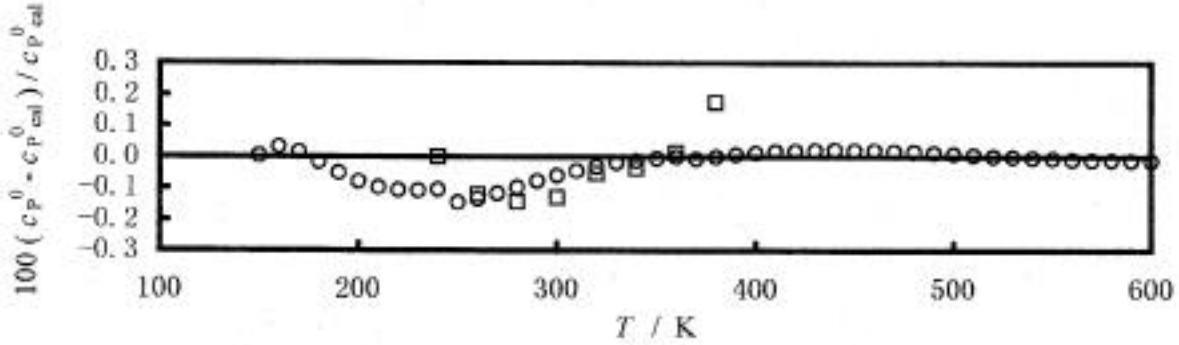
100 (c_P^0 - $c_{P\,cal}^0$) / $c_{P\,cal}^0$
0.3
0.2
0.1
0.0
−0.1
−0.2
−0.3
100
200
300
400
500
600
T / K

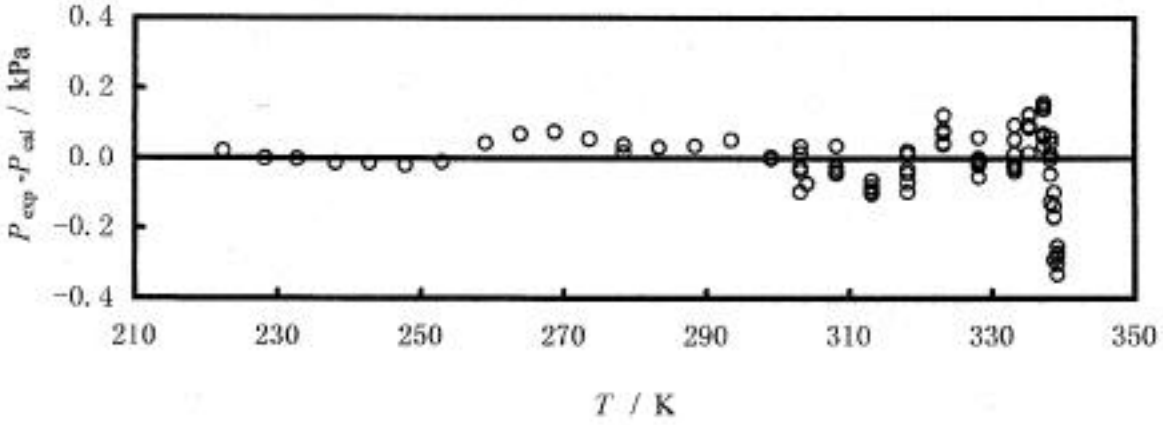
0.4
0.2
0.0
−0.2
−0.4
P_{exp}-P_{cal} / kPa
210
230
250
270
290
310
330
350
T / K

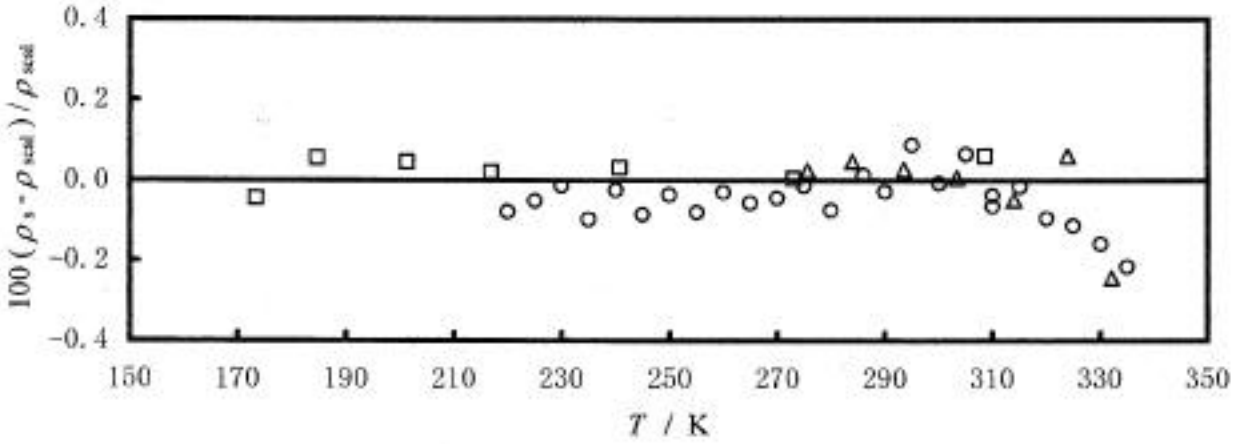
0.4
0.2
0.0
−0.2
−0.4
100 (ρs - ρscal) / ρscal
150
170
190
210
230
250
270
290
310
330
350
T / K

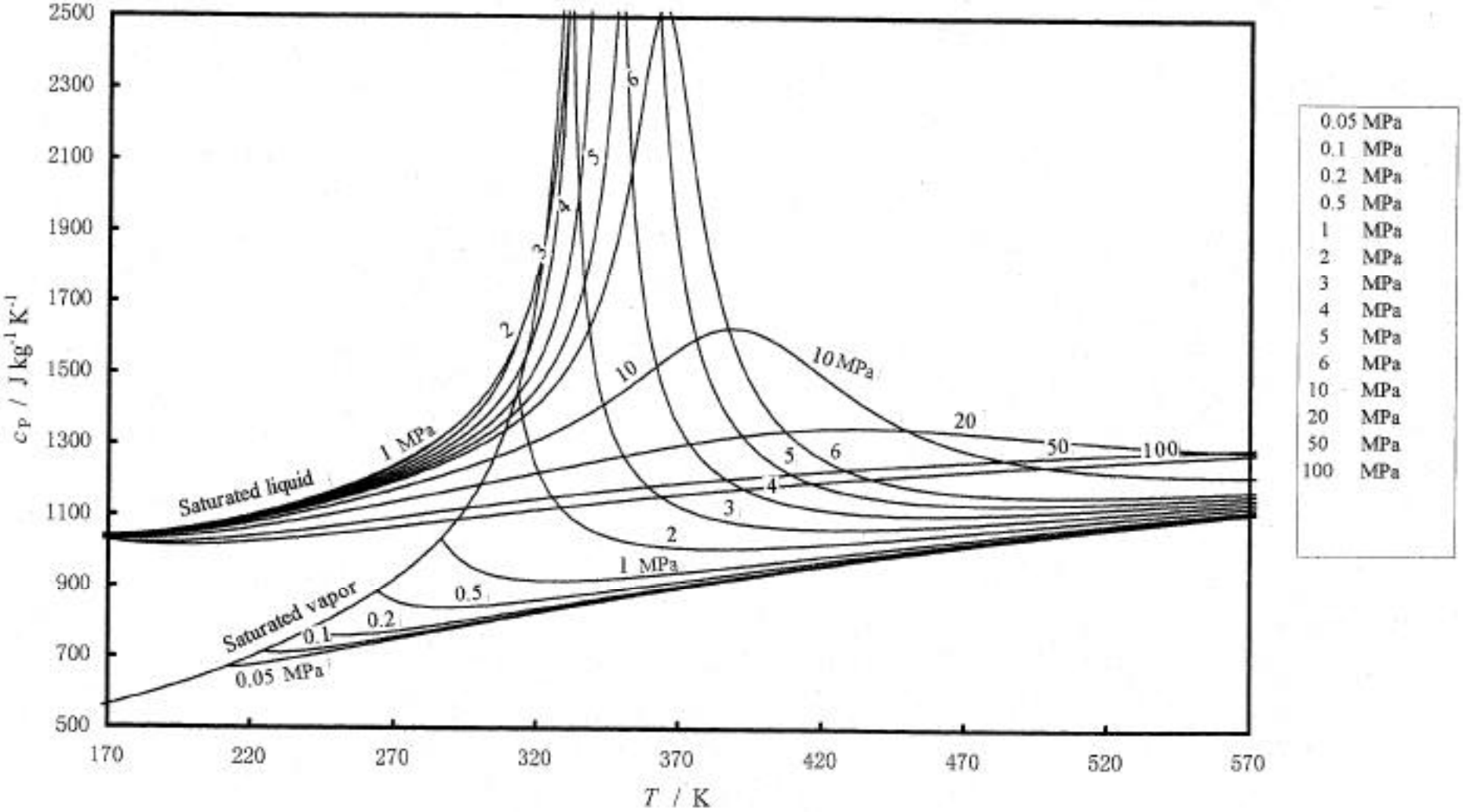
2500
2300
2100
1900
1700
1500
1300
1100
900
700
500
c_P / J kg^{-1} K^{-1}
170
220
270
320
370
420
470
520
570
T / K
Saturated liquid
Saturated vapor
1 MPa
2
3
4
5
6
10
10 MPa
20
50
100
0.5
0.2
0.1
0.05 MPa
0.05 MPa
0.1 MPa
0.2 MPa
0.5 MPa
1 MPa
2 MPa
3 MPa
4 MPa
5 MPa
6 MPa
10 MPa
20 MPa
50 MPa
100 MPa

Fig. 6

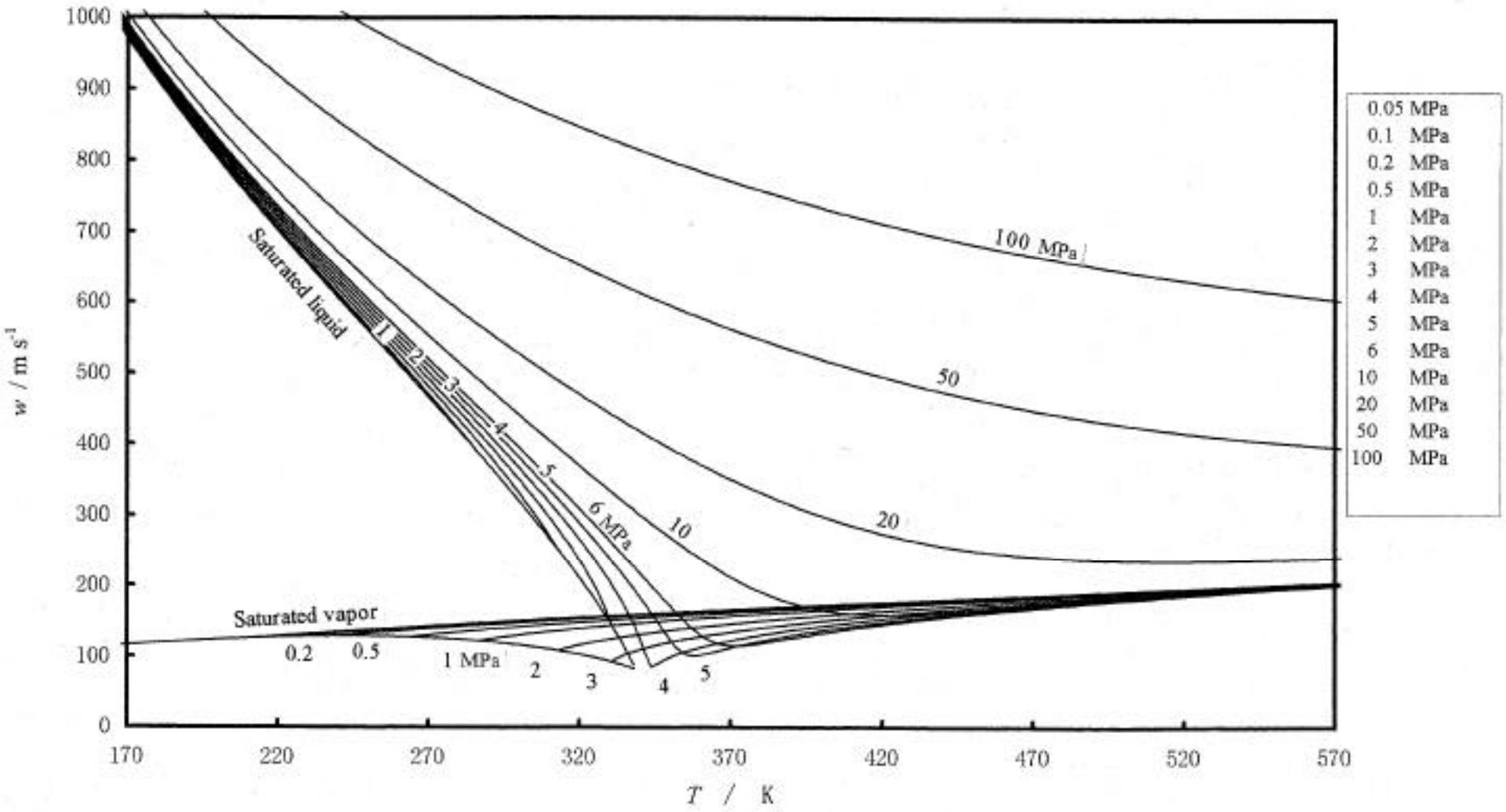
1000
900
800
700
600
500
400
300
200
100
0
w / m s-1
170
220
270
320
370
420
470
520
570
T / K
Saturated liquid
Saturated vapor
100 MPa
50
20
10
6 MPa
5
4
3
2
1
0.2
0.5
1 MPa
2
3
4
5
0.05 MPa
0.1 MPa
0.2 MPa
0.5 MPa
1 MPa
2 MPa
3 MPa
4 MPa
5 MPa
6 MPa
10 MPa
20 MPa
50 MPa
100 MPa

Fig. 7